Figure S1

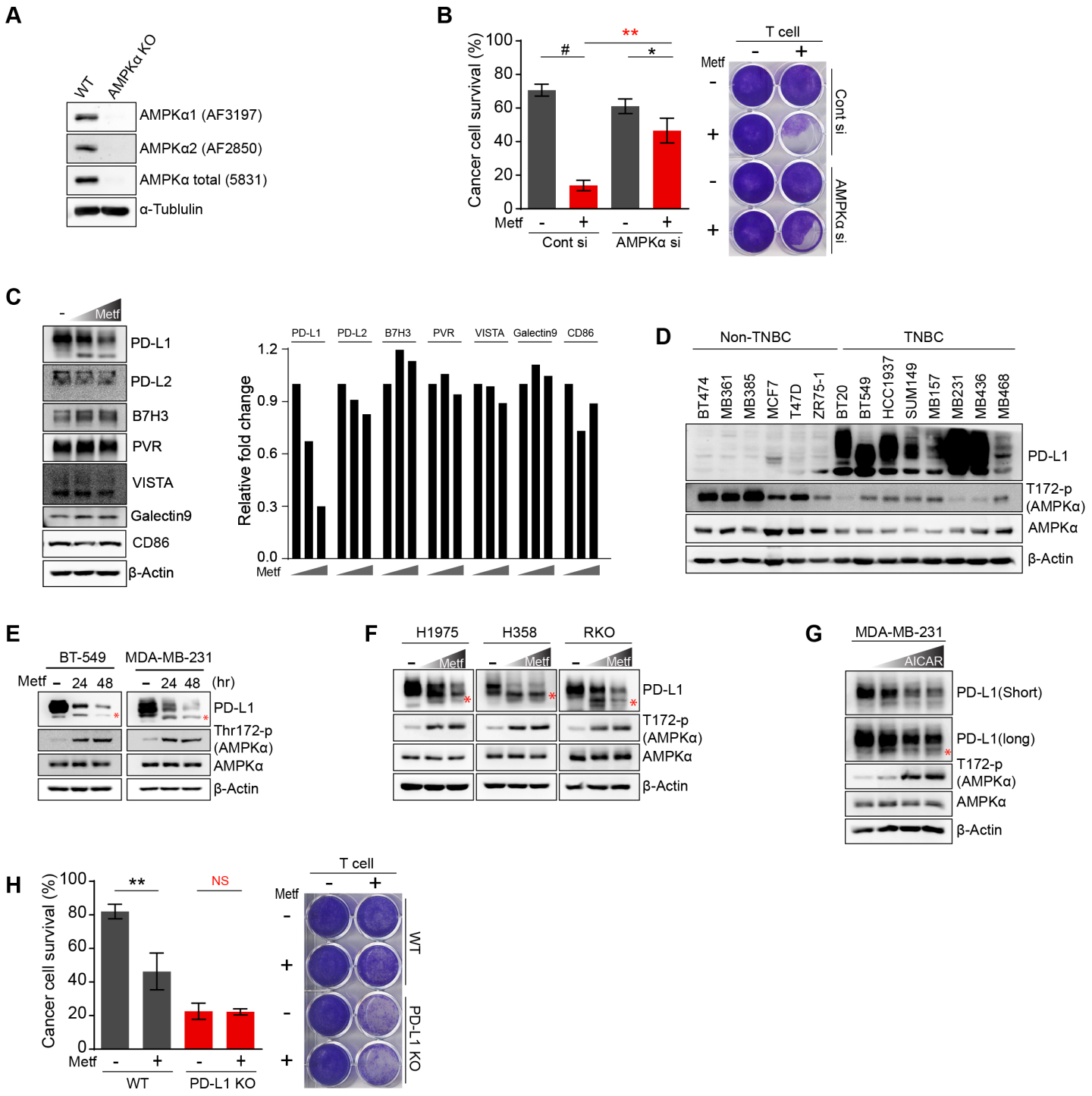
A
WT
AMPKα KO
AMPKα1 (AF3197)
AMPKα2 (AF2850)
AMPKα total (5831)
α-Tublulin
B
Cancer cell survival (%)
100
80
60
40
20
0
**
#
*
Metf
-
+
Cont si
AMPKα si
T cell
Cont si
AMPKα si
C
Metf
PD-L1
PD-L2
B7H3
PVR
VISTA
Galectin9
CD86
β-Actin
Relative fold change
1.2
0.9
0.6
0.3
0.0
D
Non-TNBC
TNBC
BT474
MB361
MB385
MCF7
T47D
ZR75-1
BT20
BT549
HCC1937
SUM149
MB157
MB231
MB436
MB468
PD-L1
T172-p (AMPKα)
AMPKα
β-Actin
E
BT-549
MDA-MB-231
Metf
24
48
(hr)
PD-L1
Thr172-p (AMPKα)
AMPKα
β-Actin
F
H1975
H358
RKO
Metf
PD-L1
T172-p (AMPKα)
AMPKα
β-Actin
G
MDA-MB-231
AICAR
PD-L1(Short)
PD-L1(long)
T172-p (AMPKα)
AMPKα
β-Actin
H
Cancer cell survival (%)
100
80
60
40
20
0
**
NS
Metf
WT
PD-L1 KO
T cell
WT
PD-L1 KO

Figure S1 (related to Figure 1). Metformin increases CTL activity through the AMPK/PD-L1 axis. (A) Both AMPKα1 and α2 were knocked-out in MDA-MB-231 cell. **(B)** T cell-mediated cancer cell killing assay. BT-549 cells co-cultured with activated T cells for 48 hours in the presence or absence of metformin (5 mM) were subjected to crystal violet staining to determine cell viability. AMPKα was knocked down by siRNA transfection. BT-549 transfectants to T-cell ratio, 1:5. Data represent mean ± S.D. n = 3. **(C)** MDA-MB-231 cells were treated with metformin (2.5 mM and 5 mM) for 24 hours. The signal intensity of each proteins were quantified using Image J program and then normalized the signal intensity to that of β-actin. Normalized expression levels were shown as fold change over negative control. **(D)** The expression of AMPKα, AMPKα T172-p, and PD-L1 was examined in fourteen different breast cell lines by immunoblotting. Correlation analysis shown in Figure 1G. **(E)** BT-549 and MDA-MB-231 breast cancer cells were treated with metformin (5 mM) for 24 to 48 hours. Asterisk, PD-L1 band shift. **(F)** Non-small cell lung cancer (H1975 and H358) and colon cancer (RKO) cells were treated with metformin (2.5 mM and 5 mM) for 24 hours. Asterisk, PD-L1 band shift. **(G)** MDA-MB-231 cells were treated with increasing concentrations of AMPK activator, 5-aminoimidazole-4-carboxamide ribonucleotide (AICAR; 250 μM, 500 μM, and 1 mM) for 24 hours. Asterisk, PD-L1 band shift. **(H)** T cell-mediated cancer cell killing assay. WT or PD-L1 KO BT-549 cells to T-cell ratio, 1:3. Data represent mean ± S.D. n = 3. **P*, 0.01~0.05, ***P*, 0.001~0.01, $^{\#}P$, < 0.001, and NS, not significant, Student's *t*-test.

Figure S2

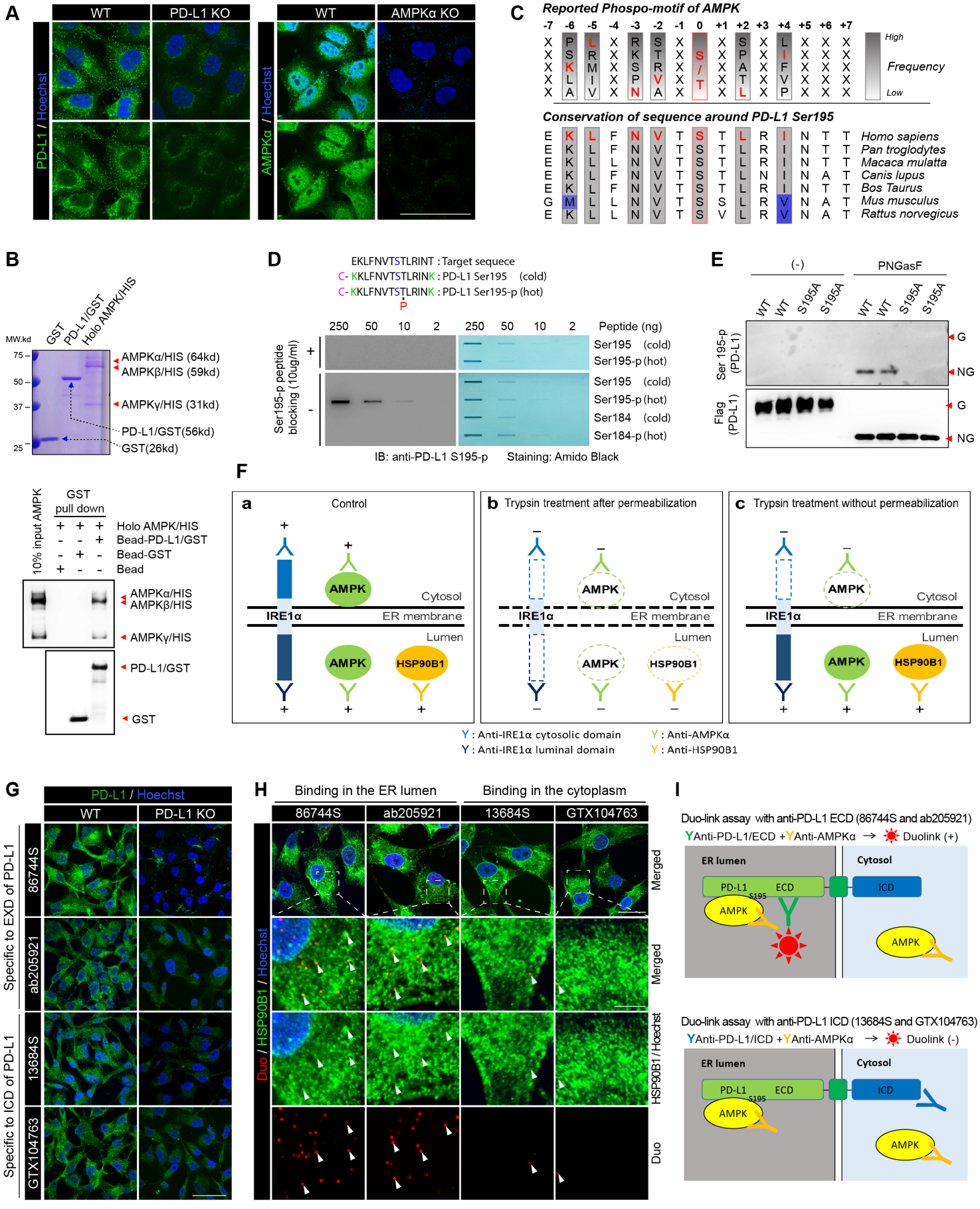
A
WT
PD-L1 KO
AMPKα KO
PD-L1 / Hoechst
AMPKα / Hoechst
C
Reported Phospo-motif of AMPK
-7 -6 -5 -4 -3 -2 -1 0 +1 +2 +3 +4 +5 +6 +7
High
Frequency
Low
Conservation of sequence around PD-L1 Ser195
Homo sapiens
Pan troglodytes
Macaca mulatta
Canis lupus
Bos Taurus
Mus musculus
Rattus norvegicus
B
MW.kd
GST
PD-L1/GST
Holo AMPK/HIS
AMPKα/HIS (64kd)
AMPKβ/HIS (59kd)
AMPKγ/HIS (31kd)
PD-L1/GST(56kd)
GST(26kd)
10% input AMPK
GST pull down
Holo AMPK/HIS
Bead-PD-L1/GST
Bead-GST
Bead
AMPKα/HIS
AMPKβ/HIS
AMPKγ/HIS
PD-L1/GST
GST
D
EKLFNVTSTLRINT : Target sequece
C- KKLFNVTSTLRINK : PD-L1 Ser195 (cold)
C- KKLFNVTSTLRINK : PD-L1 Ser195-p (hot)
Peptide (ng)
Ser195-p peptide blocking (10ug/ml)
Ser195 (cold)
Ser195-p (hot)
Ser184 (cold)
Ser184-p (hot)
IB: anti-PD-L1 S195-p
Staining: Amido Black
E
(-)
PNGasF
WT
S195A
Ser 195-p (PD-L1)
Flag (PD-L1)
G
NG
F
a Control
b Trypsin treatment after permeabilization
c Trypsin treatment without permeabilization
AMPK
Cytosol
IRE1α
ER membrane
Lumen
HSP90B1
Y : Anti-IRE1α cytosolic domain
Y : Anti-IRE1α luminal domain
Y : Anti-AMPKα
Y : Anti-HSP90B1
G
PD-L1 / Hoechst
WT
PD-L1 KO
Specific to EXD of PD-L1
86744S
ab205921
Specific to ICD of PD-L1
13684S
GTX104763
H
Binding in the ER lumen
Binding in the cytoplasm
86744S
ab205921
13684S
GTX104763
Duo / HSP90B1 / Hoechst
Merged
HSP90B1 / Hoechst
Duo
I
Duo-link assay with anti-PD-L1 ECD (86744S and ab205921)
YAnti-PD-L1/ECD +YAnti-AMPKα → Duolink (+)
ER lumen
Cytosol
PD-L1
ECD
ICD
S195
AMPK
Duo-link assay with anti-PD-L1 ICD (13684S and GTX104763)
YAnti-PD-L1/ICD +YAnti-AMPKα → Duolink (-)

Figure S2 (related to Figure 2). AMPK activated by metformin directly phosphorylates serine 195 of PD-L1. (A) Validation of the specificity of the AMPK and PD-L1 antibodies (used in Duolink assay in Figure 2A) for immunofluorescence staining. MDA-MB-231 WT, PD-L1 KO and AMPKα KO cells were subjected to immunofluorescence staining with the indicated antibodies. Scale bar, 50 μm. **(B)** AMPK binds directly to PD-L1 *in vitro*. Top, The purity of purified proteins for GST-pull down assay was examined by Coomassie blue staining. Bottom, Glutathione beads or glutathione beads conjugated with GST or GST-PD-L1 were incubated with the holo-AMPK complex and subjected to GST pull-down assay followed by Western blotting with the indicated antibodies. **(C)** AMPK phospho-motif of PD-L1 and conservative sequence around Ser195. Top, phospho-motif based on 64 validated sites phosphorylated by AMPK. Bottom, Sequence alignment of the PD-L1 S195 region in different species. **(D, E)** Characterization of the S195-p antibody. **(D)** Top, The sequence of cold and hot peptides. The 5′ and 3′ terminal amino acids were replaced with lysine to increase the solubility of the peptides. Bottom, The specificity of the S195-p antibody was examined with dot blotting. The S195-p antibody specifically bind with the hot peptide (S195-p) while not binding with the cold peptide (S195) and the other hot peptide (S184-p) for the phosphorylation site. Such specific reaction of the S195-p antibody was completed neutralized by blocking with excessive amount of the hot peptide (S195-p). Amino black staining was performed to show peptides on the nitrocellulose membrane. **(E)** *In vivo* phosphorylation of PD-L1 S195. Immunoblotting was performed with PDL1 S195-p antibody after removing glycan structure with PNGase F reaction following IP. G: glycosylated form. NG: non-glycosylated form. **(F)** Model illustrating trypsinization of the ER fractions in Figure 2l. (a) ER fraction without trypsin. All markers were detected. (b) ER fraction subjected to trypsin digestion with permeabilization (1% Triton X-100, 3 min). No markers were detected. (c) ER fraction subjected to trypsin digestion without permeabilization. Cytosolic portions of ER proteins were not detected after digestion whereas luminal portions of ER proteins were detected. **(G)** The indicated antibodies were verified for IF staining in parental BT-549 and PD-L1 KO BT-549 cells. All five antibodies are specific for PD-L1 and available for IF staining. Scale bar, 50 μm. **(H)** Duolink II assay (AMPK/PD-L1) combined with ER marker staining. Each antibodies specific for the extracelluar (86744S and Ab205921) and intracellular (13684S and GTX104763) domain of PD-L1 were subjected to Duolink II assay together with antibody specific for AMPKα. Immediately after the Duolink procedure, the samples were immunostained with antibody specific for ER (HSP90B1) and nuclei were stained with Hoechst. Scale bar, 20 μm (inset, 5 μm) **(I)** Model illustrating Duolink II assay in Figure 2K and S2H.

Figure S3

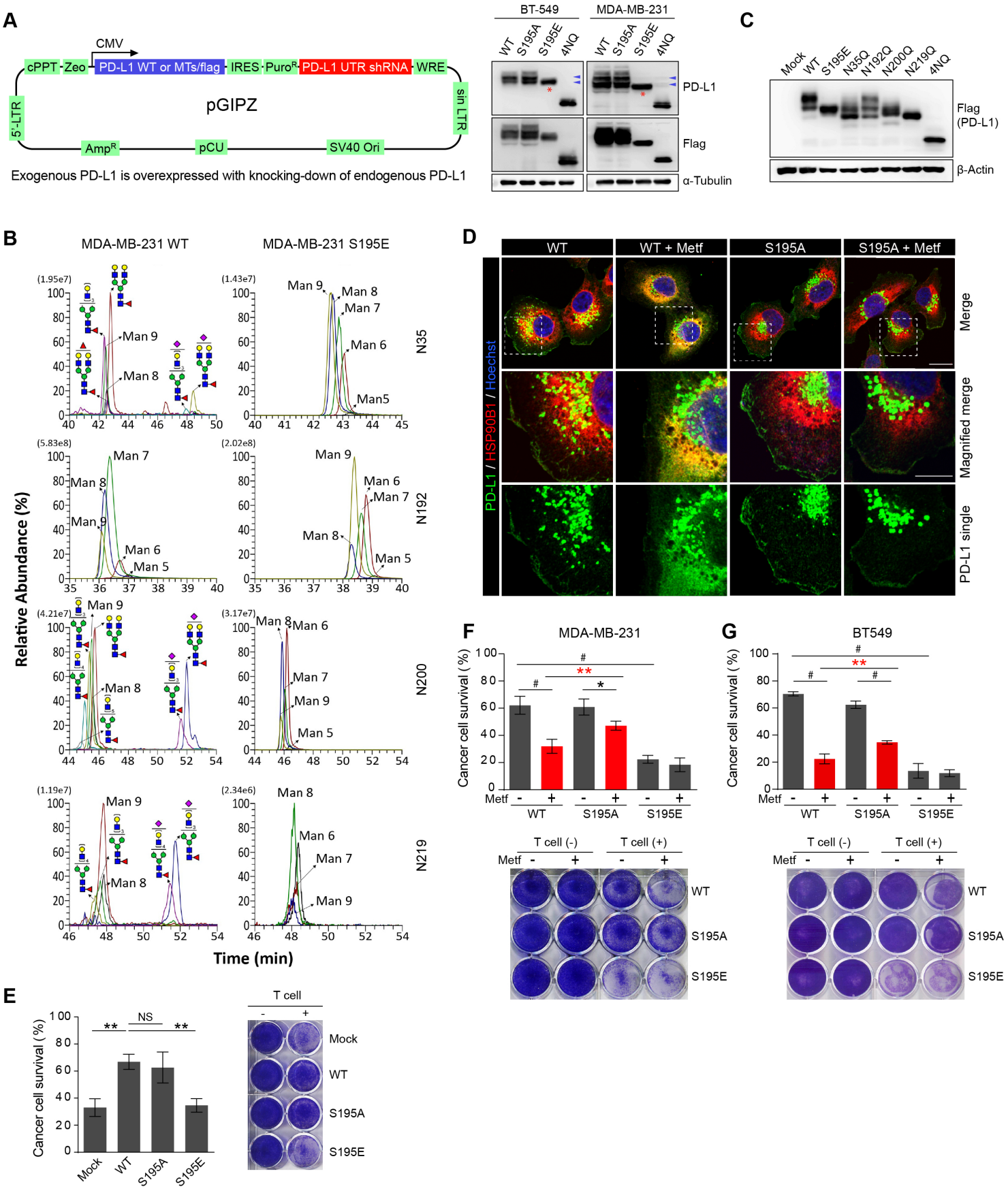
A
CMV
cPPT
Zeo
PD-L1 WT or MTs/flag
IRES
Puro^R
PD-L1 UTR shRNA
WRE
5'-LTR
pGIPZ
sin LTR
Amp^R
pCU
SV40 Ori
Exogenous PD-L1 is overexpressed with knocking-down of endogenous PD-L1
BT-549
MDA-MB-231
WT
S195A
S195E
4NQ
PD-L1
Flag
α-Tubulin
C
Mock
WT
S195E
N35Q
N192Q
N200Q
N219Q
4NQ
Flag (PD-L1)
β-Actin
B
MDA-MB-231 WT
MDA-MB-231 S195E
Relative Abundance (%)
Time (min)
N35
N192
N200
N219
Man 9
Man 8
Man 7
Man 6
Man5
Man 5
D
WT
WT + Metf
S195A
S195A + Metf
PD-L1 / HSP90B1 / Hoechst
Merge
Magnified merge
PD-L1 single
F
MDA-MB-231
Cancer cell survival (%)
Metf
WT
S195A
S195E
T cell (-)
T cell (+)
G
BT549
E
T cell
Mock
NS

Figure S3 (related to Figure 3). Phosphorylation of PD-L1 S195 induces its abnormal glycosylation and blocks its ER-to-Golgi translocation. (A) Generation of stable cell lines expressing wild type and mutant PD-L1. Left, A dual expression p-GIPZ vector was used to generate stable cell line. The lentiviral-based sh RNA (pGIPZ), which contains the shRNA sequence targeting 3′UTR of human PD-L1, was used as the template. The original cDNA for GFP was replaced with cDNA for Flag-PD-L1 WT, S195A, S195E or 4NQ. Right, PD-L1 level was examined by immunoblotting with antibody against PD-L1 and Flag. Exogenous PD-L1 (Flag) was overexpressed and endogenous PD-L1 (PD-L1) was knocked down (4NQ_blue arrow). Asterisk, PD-L1 band shift. **(B)** LC-MS/MS-based identification of N-glycopeptides. Comparative profiling of N-glycopeptides derived from WT and S195E PDL1 expressed in MDA-MB-231 cells. The extracted ion chromatograms (by theoretical m/z values at 6 ppm mass accuracy) of the most abundant N-glycopeptides for the WT and all those identified for S195E PDL1 at each of the four sites were overlaid and normalized to the highest glycopeptide peak intensity, the absolute values of which were shown in parentheses. **(C)** The expression of WT, S195E, and NXT motif mutant PD-L1. PD-L1 band shift can be observed. **(D)** PD-L1 localization in MDA-MB-231 WT and S195A PD-L1 stable cells was examined by immunofluorescence staining after metformin (5 mM) treatment for 24 hours. MG132 (10 μM) was added 6 hours prior to fixation to prevent degradation of PD-L1. Hoechst was used for nuclear counter staining. Scale bar, 20 μm (inset, 10 μm). **(E)** The effects of WT, S195A and S195E PD-L1 on T-cell killing activity. MDA-MB-231 mock, WT, S195A, or S195E PD-L1 stable cells were co-cultured with activated T cells for 48 hours. Cell viability was assessed by crystal violet staining and quantified. Cancer cell to T-cell ratio, 1:10. Mean ± S.D.; n=3 **(F)** T cell-mediated cancer cell killing assay. MDA-MB-231 WT, S195A or S195E PD-L1 stable cells were co-cultured with activated T cell for 48 hours in the presence or absence of metformin (5 mM). The ratio of cancer cells to T cells was 1:10. Data represent mean ± S.D. n =3. **(G)** WT, S195A or S195E PD-L1 BT-549 stable cells to T-cell ratio, 1:10. Data represent mean ± S.D. n = 3. **P*, 0.01~0.05, ***P*, 0.001~0.01, $^{\#}P$, < 0.001, and NS, not significant, Student's *t*-test.

Figure S4

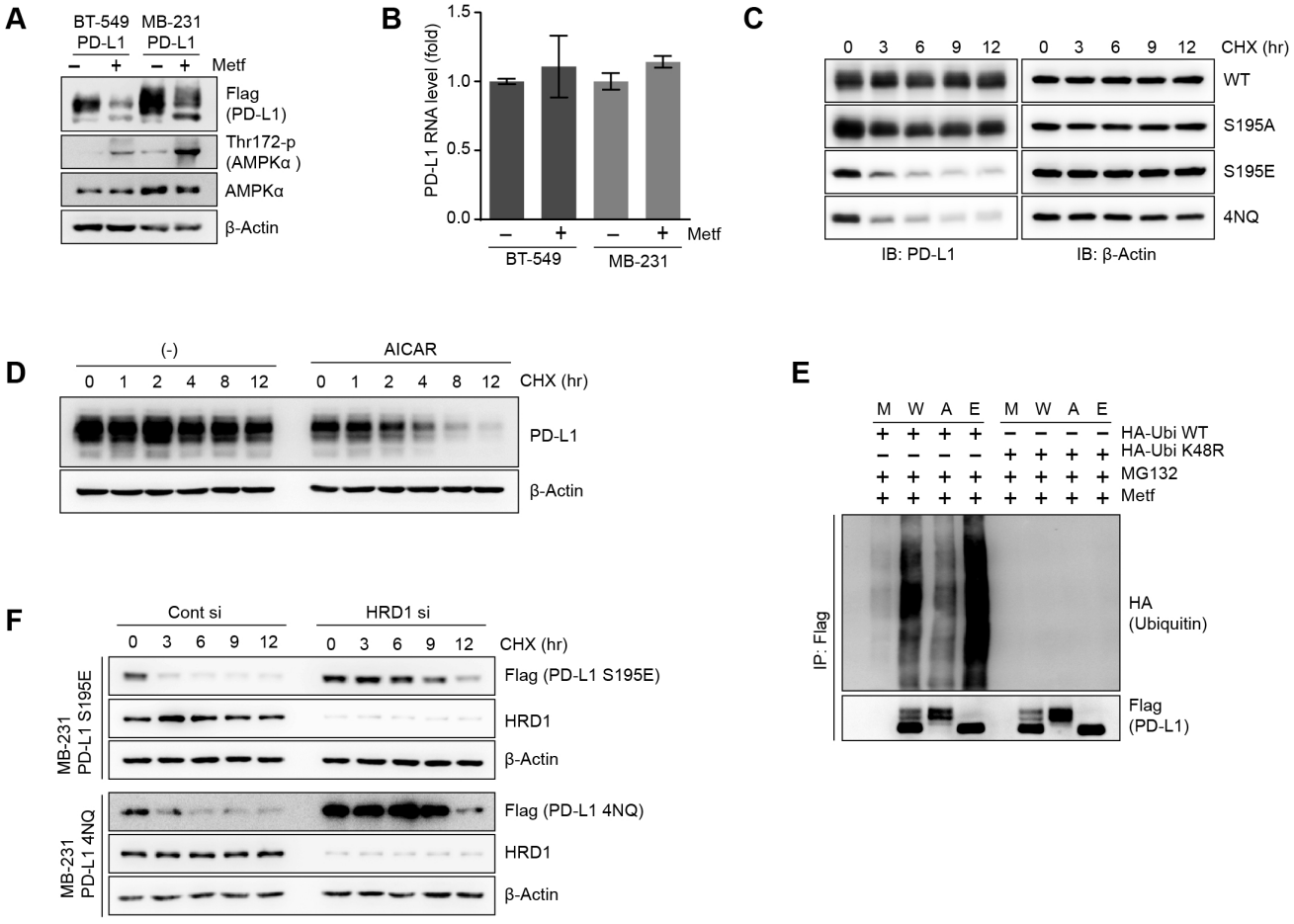
A
BT-549 PD-L1
MB-231 PD-L1
Metf
Flag (PD-L1)
Thr172-p (AMPKα)
AMPKα
β-Actin
B
PD-L1 RNA level (fold)
1.5
1.0
0.5
0.0
BT-549
MB-231
Metf
C
CHX (hr)
0 3 6 9 12
WT
S195A
S195E
4NQ
IB: PD-L1
IB: β-Actin
D
(-)
AICAR
0 1 2 4 8 12
CHX (hr)
PD-L1
β-Actin
E
M W A E
HA-Ubi WT
HA-Ubi K48R
MG132
Metf
IP: Flag
HA (Ubiquitin)
Flag (PD-L1)
F
Cont si
HRD1 si
0 3 6 9 12
CHX (hr)
MB-231 PD-L1 S195E
Flag (PD-L1 S195E)
HRD1
β-Actin
MB-231 PD-L1 4NQ
Flag (PD-L1 4NQ)
HRD1
β-Actin

Figure S4 (related to Figure 4). Phosphorylation of S195 induces ER-associated degradation of PD-L1. (A) BT549 and MDA-MB-231 (MB-231) cells expressing exogenous WT PD-L1 were treated with metformin (5 mM) for 24 hours and subjected to Western blotting with the indicated antibodies. **(B)** Parental BT549 and MDA-MB-231 (MB-231) cells were treated with metformin (5 mM) for 24 hours and subjected to real-time PCR assay to detect PD-L1 RNA levels. **(C)** Protein stability of WT, S195A, S195E, and non-glycosylated (4NQ) PD-L1. Each stable cell line was treated with protein synthesis inhibitor cycloheximide (CHX, 50 μM) for the indicated time and subjected to Western blotting with PD-L1 antibody. **(D)** MDA-MB-231 were treated with AICAR (1mM) for 24 hours and then, treated with CHX (50 μM) for the indicated time. **(E)** MDA-MB-231 stable cells expressing exogenous WT or K48R mutant HA-tagged ubiquitin (non-polymerization) were treated or without metformin (5 mM) for 24 hours followed by MG132 (10 μM) for 6 hours. Ubiquitination of WT, S195A, and S195E PD-L1 was examined by HA immunoblotting after IP with Flag M2 magnetic bead. M, mock. W, WT PD-L1. A, S195A PD-L1. E, S195E PD-L1. **(F)** Control or HRD1 siRNA was transfected into MDA-MB-231 stable cells expressing exogenous 4NQ or S195E. The stability of 4NQ and S195E PD-L1 was examined after treatment of CHX (50 μM) for the indicated time.

Figure S5

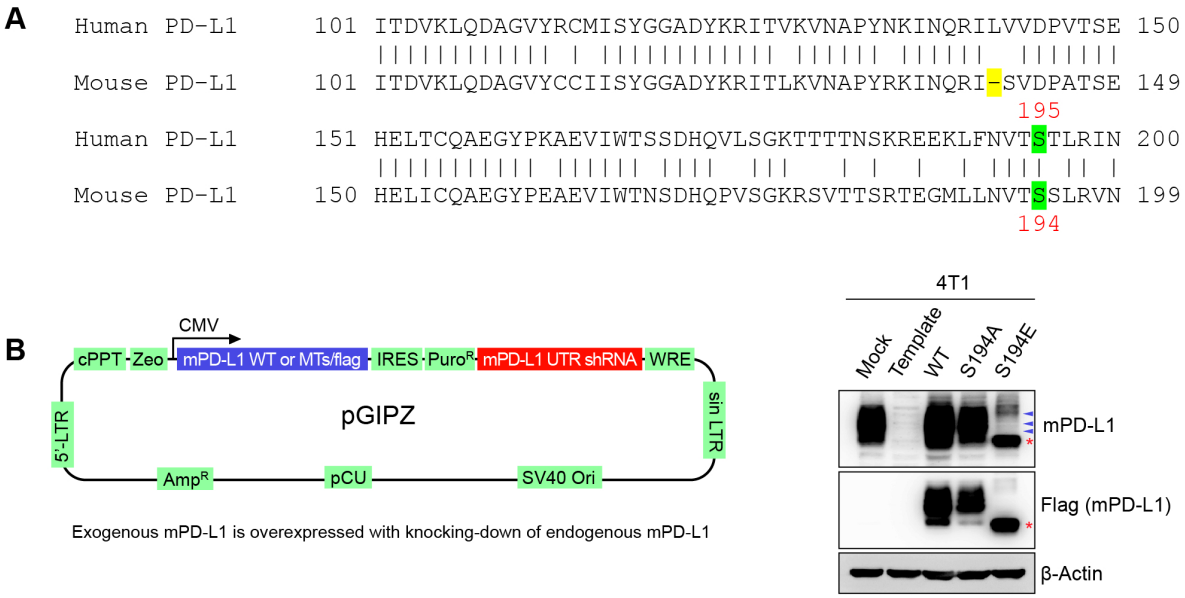
A
Human PD-L1 101 ITDVKLQDAGVYRCMISYGGADYKRITVKVNAPYNKINQRILVVDPVTSE 150
Mouse PD-L1 101 ITDVKLQDAGVYCCIISYGGADYKRITLKVNAPYRKINQRI-SVDPATSE 149
195
Human PD-L1 151 HELTCQAEGYPKAEVIWTSSDHQVLSGKTTTTNSKREEKLFNVTSTLRIN 200
Mouse PD-L1 150 HELICQAEGYPEAEVIWTNSDHQPVSGKRSVTTSRTEGMLLNVTSSLRVN 199
194
B
CMV
cPPT
Zeo
mPD-L1 WT or MTs/flag
IRES
Puro^R
mPD-L1 UTR shRNA
WRE
5'-LTR
pGIPZ
sin LTR
Amp^R
pCU
SV40 Ori
Exogenous mPD-L1 is overexpressed with knocking-down of endogenous mPD-L1
4T1
Mock
Template
WT
S194A
S194E
mPD-L1
Flag (mPD-L1)
β-Actin
C
4T1
WT
S194A
S194E
PD-L1 / HSP90B1 / Hoechst
Merge
HSP90B1
Hoechst
PD-L1 single

Figure S5 (related to Figure 5). The reduction of PD-L1 by metformin-activated AMPK is physiologically significant and clinically relevant. (A) Sequence homology analysis between human and mouse. **(B)** Generation WT, S194A and S194E PD-L1 4T1 stable cells. Left, A dual expression p-GIPZ vector was used to generate stable cell line. The lentiviral-based sh RNA (pGIPZ), which contains the shRNA sequence targeting 3′UTR of mouse (m) PD-L1, was used as the template. The original cDNA for GFP was replaced with cDNA for Flag-mPD-L1 WT, S194A, or S195E. Right, PD-L1 level was examined by immunoblotting with antibody against mPD-L1 and Flag. Exogenous mPD-L1 (Flag) was overexpressed and endogenous mPD-L1 (PD-L1) was knocked down (S194E_blue arrow). Asterisk, PD-L1 band shift. **(C)** Subcellular localization of WT, S194A, or S194E mPD-L1. Each stable cell line was immunostained with an antibody against Flag (PD-L1) and HSP90B1 (ER marker). The nuclei were stained with Hoechst. Scale bar 20 μm.

Figure S6

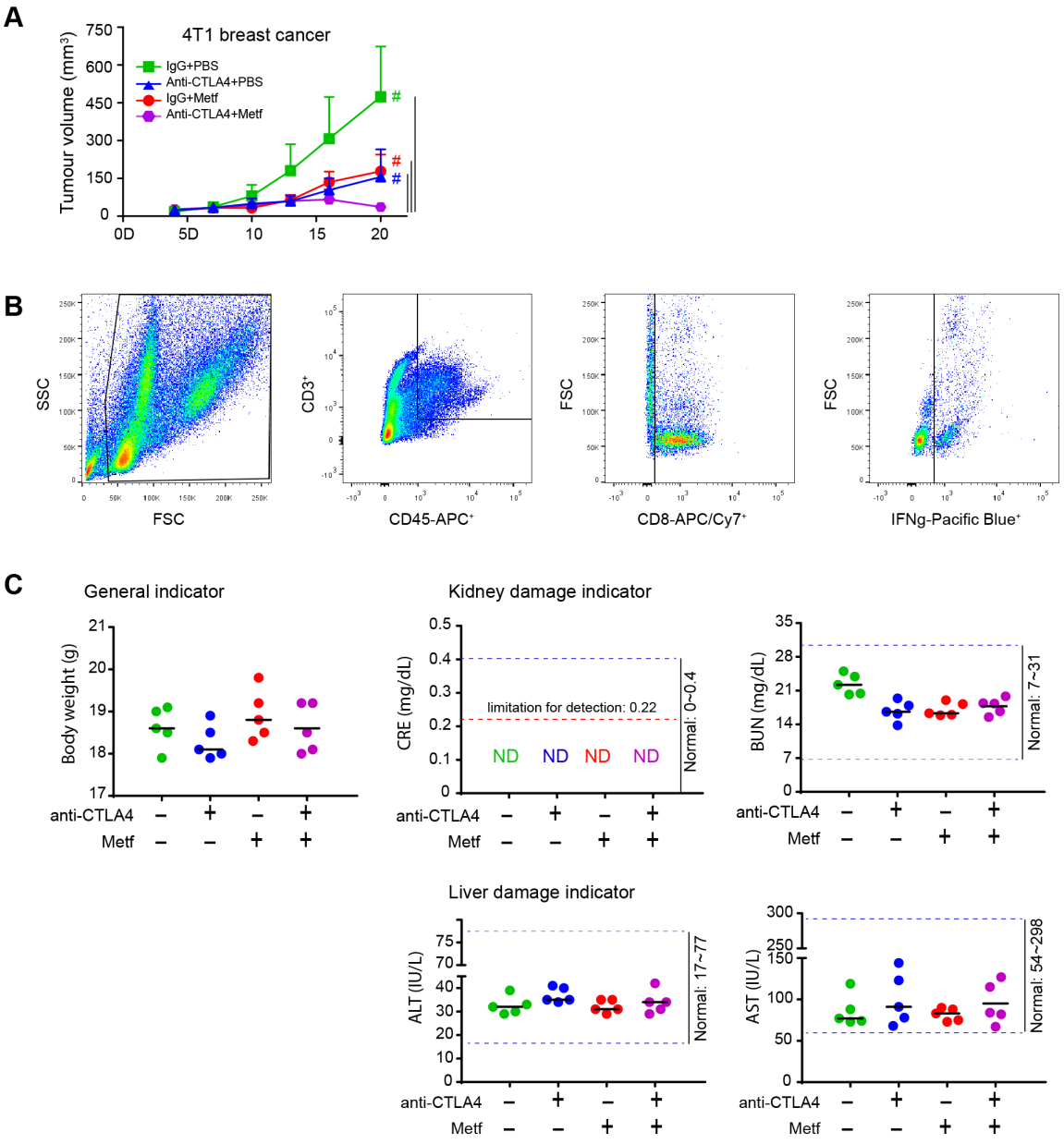
A
4T1 breast cancer
IgG+PBS
Anti-CTLA4+PBS
IgG+Metf
Anti-CTLA4+Metf
Tumour volume (mm³)
0D
5D
10
15
20
#
B
SSC
FSC
CD3⁺
CD45-APC⁺
FSC
CD8-APC/Cy7⁺
FSC
IFNg-Pacific Blue⁺
C
General indicator
Body weight (g)
Kidney damage indicator
CRE (mg/dL)
limitation for detection: 0.22
ND
Normal: 0~0.4
BUN (mg/dL)
Normal: 7~31
Liver damage indicator
ALT (IU/L)
Normal: 17~77
AST (IU/L)
Normal: 54~298
anti-CTLA4
Metf

Figure S6 (related to Figure 6). The combination of metformin and CTLA4 blockade effectively suppresses tumor growth *in vivo*. (A) Combined treatment of metformin and CTLA-4 antibody effectively inhibits tumor growth**.** 4T1-Luc2 cells (5×10^4) in 50 μL of medium mixed with 50 μL of matrigel basement membrane matrix (BD Biosciences, San Jose, CA, USA) were injected into the mammary fat pad of 6-week-old female BALB/c mice. Four days after inoculation, mice were treated daily with metformin (200 mg/kg in 100 μL PBS) by oral gavage until end point. CTLA-4 antibody (100 μg/100 μL, Bio X Cell) or control hamster IgG (100 μg/100 μL, Bio X Cell) was administered to mice by i.p. injection on day 7, 10, and 13 after inoculation. Tumor size was measured at the indicated time points and tumor volume calculated by using the formula: $\pi/6 \times \text{length} \times \text{width}^2$. **(B)** Live cells in leukocyte fraction were gated via FSC and SSC. After exclusion of dead cells, T-cell population was gated based on the surface expression of CD45 and CD3. $CD8^+$ CTL population was gated based on surface expression of CD8. Activation of CTL was evaluated by intracellular IFN-γ intensity. Quantitation shown in Figure 6F. **(C)** Analysis of liver and kidney function indicators in mice treated with metformin, anti-CTLA4, or the combination. Body weight and kidney/liver function indicators in mice with 4T1-derived tumors after each indicated treatment. Data represent mean ± S.D. n=5 mice per group. Normal range indicated by the dashed lines.

protein	mass	pI	exp_mz	exp_mr	exp.z	calc_mr	delta	score	sequence	position
PD-L1-flag	34647	6.16	453.5	1357.6	3	1357.6	-0.0001	24	KCGIQD**T**N**S**KK	Thr277 or Ser279
PD-L1-flag	34647	6.16	1067.9	2133.8	2	2133.8	-0.0043	28	Q**S**D**T**HLEETDYKDDDDK	Ser283 or Thr285
PD-L1-flag	34647	6.16	572.8	1143.6	2	1143.6	0.0003	20	LFNVT**S**TLR	Ser195

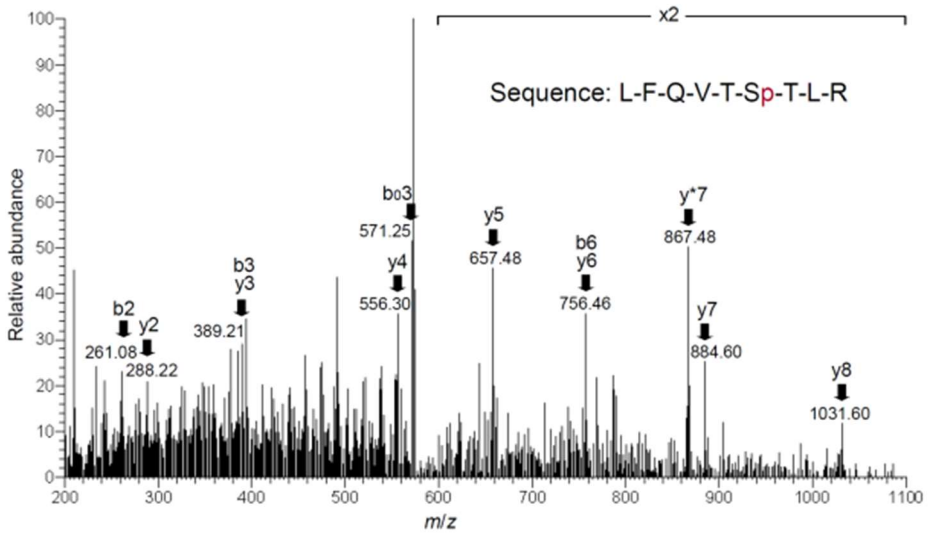

Table S1 (related to Figure 2). Detection of Ser/Thr phosphorylation of PD-L1 by IP / MS analysis. PD-L1-flag was immunoprecipitated from the lysate of BT549 WT PD-L1 stable cell using Flag M2 bead, purified through gel elution after electrophoresis, and subjected to LC-MS/MS analysis to identify the phosphorylation sites

Site	Peptide Sequence [1]	Glycan Composition [2]	m/z [3]	z	BT549 WT	BT549 S195E	MB231 WT	MB231 S195E	293T WT	293T S195E
N35	DLYVVEYGSNMTIECK	HexNAc2Hex5	1051.7684	3		+		+		+
		HexNAc2Hex6	1105.7860	3		+		+		+
		HexNAc2Hex7	1159.8036	3		+		+		+
		HexNAc4Hex5	1187.1546	3	+					
		HexNAc2Hex8	1213.8212	3	+	+	+	+	+	+
		dHex1HexNAc4Hex5	1235.8406	3	+		+			
		dHex1HexNAc5Hex4	1249.5161	3					+	
		HexNAc2Hex9	1267.8388	3	+	+	+	+	+	+
		dHex2HexNAc4Hex5	1284.5266	3	+		+			
		dHex1HexNAc5Hex5	1303.5337	3					+	
		dHex1HexNAc5Hex6	1357.5513	3	+		+			
		dHex1HexNAc4Hex5NeuAc	1332.8724	3			+			
		dHex1HexNAc6Hex6	1425.2445	3					+	
		dHex1HexNAc5Hex6NeuAc	1454.5831	3			+			
		dHex1HexNAc7Hex7	1546.9552	3					+	
N192	LFNVTSTLR	HexNAc2Hex5	1134.0124	2	+		+		+	
		HexNAc2Hex6	1215.0388	2	+		+		+	
		HexNAc2Hex7	1296.0652	2	+		+		+	
		HexNAc3Hex6	1316.5785	2	+				+	
		HexNAc2Hex8	1377.0916	2	+		+		+	
		HexNAc2Hex9	1458.1180	2	+		+		+	
	LFNVTETLR	HexNAc2Hex5	1155.0177	2		+		+		+
		HexNAc2Hex6	1236.0441	2		+		+		+
		HexNAc2Hex7	1317.0705	2		+		+		+
		HexNAc2Hex8	1398.0969	2		+		+		+
		HexNAc2Hex9	1479.1233	2		+		+		+
N200	INTTTNEIFYCTFR	HexNAc2Hex5	999.4252	3		+		+		+
		HexNAc2Hex6	1053.4428	3		+		+		+
		HexNAc2Hex7	1107.4604	3		+		+		+
		HexNAc2Hex8	1161.4780	3	+	+	+	+	+	+
		dHex1HexNAc4Hex5	1183.4974	3	+		+		+	
		HexNAc2Hex9	1215.4956	3	+	+	+	+	+	+
		dHex1HexNAc5Hex5	1251.1905	3					+	
		dHex1HexNAc4Hex5NeuAc	1280.5292	3	+		+			
		dHex1HexNAc5Hex6	1305.2081	3	+		+		+	
		dHex1HexNAc6Hex6	1372.9013	3					+	
		dHex1HexNAc5Hex6NeuAc	1402.2399	3	+		+		+	
		dHex1HexNAc6Hex7	1426.9189	3	+		+		+	
		dHex1HexNAc7Hex8	1548.6292	3	+		+			
N219	LDPEENHTAELVIPELPLAHPPN	HexNAc2Hex6	1052.9840	4		+		+		+
		HexNAc2Hex7	1093.4972	4		+		+		+
		HexNAc2Hex8	1134.0104	4		+	+	+	+	+
		HexNAc2Hex9	1174.5236	4	+	+	+	+	+	+
		dHex1HexNAc5Hex6	1241.8080	4	+		+		+	
		dHex1HexNAc6Hex6	1292.5779	4					+	
		dHex1HexNAc5Hex6NeuAc	1314.5819	4	+		+			
		dHex1HexNAc6Hex7	1333.0911	4	+		+		+	
		dHex1HexNAc7Hex7	1383.8609	4					+	
		dHex1HexNAc6Hex7NeuAc	1405.8649	4	+		+		+	
		dHex1HexNAc7Hex8	1424.3741	4	+					
		dHex1HexNAc7Hex7NeuAc	1456.6348	4	+		+		+	

Table S2 (related to Figure 3). Identified N-glycopeptides of WT and S195E PDL1 expressed in different cell lines. C: carbamidomethylated Cys; M: oxidized Met; E: S195E. Only the most abundant WT PD-L1 *N*-glycopepitdes identified are listed in this table. All identified S195E PD-L1 *N*-glycopeptides are listed. Theoretical values of m/z were calculated based on the assigned glycan composition and peptide backbone. These values were used to extract the respective ion chromatograms at MS level, as shown in Fig. 3C and Fig. S3B with a mass accuracy set at 6 ppm.